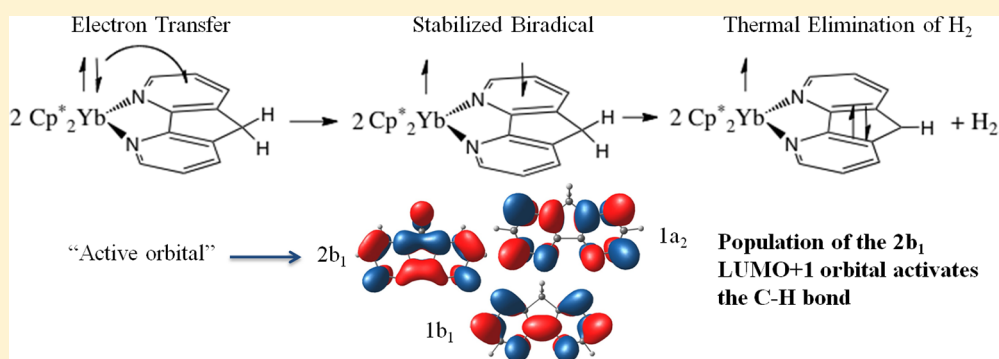


Thermal Dihydrogen Elimination from $\text{Cp}^*_2\text{Yb}(4,5\text{-diazafluorene})$ Grégory Nocton,^{†,‡,||} Corwin H. Booth,[‡] Laurent Maron,[§] and Richard A. Andersen^{*,†,‡}[†]Chemical Sciences Division, Lawrence Berkeley National Laboratory, Berkeley, California 94720, United States[‡]Department of Chemistry, University of California, Berkeley, California 94720, United States[§]LPCNO, UMR 5215, Université de Toulouse-CNRS, INSA, UPS, Toulouse, France

Supporting Information



ABSTRACT: The reaction of 4,5-diazafluorene with $\text{Cp}^*_2\text{Yb}(\text{OEt}_2)$, where Cp^* is pentamethylcyclopentadienyl, affords the isolable adduct $\text{Cp}^*_2\text{Yb}(4,5\text{-diazafluorene})$ (1), which slowly eliminates H_2 to form $\text{Cp}^*_2\text{Yb}(4,5\text{-diazafluorenyl})$ (2); the net reaction is therefore $1 \rightarrow 2 + \text{H}^\bullet$. The ytterbium atom in 1 is shown to be intermediate valent by variable-temperature L_{III} -edge X-ray absorption near-edge (XANES) spectroscopy, consistent with its low effective magnetic moment (μ_{eff}). The experimental studies are supported by complete active space self-consistent field (CASSCF) calculations, showing that two open-shell singlets lie below the triplet state. The two open-shell singlets are calculated to be multiconfigurational and closely spaced, in agreement with the observed temperature dependence of the XANES and χ data, which are fit to a Boltzmann distribution. A mechanism for dihydrogen formation is proposed on the basis of kinetic and labeling studies to involve the bimetallic complex $(\text{Cp}^*_2\text{Yb})_2(4,5\text{-diazafluorenyl})_2$, in which the heterocyclic amine ligands are joined by a carbon–carbon bond at C(9)–C(9').

INTRODUCTION

The 2,2'-bipyridine adduct of decamethylytterbocene, $(\text{C}_5\text{Me}_5)_2\text{Yb}(\text{bipy})$, and related adducts with heterocyclic amine ligands are classified as intermediate-valence compounds.¹ Thus, the valence of ytterbium in the Cp^*_2Yb fragment is neither Yb(II) nor Yb(III); rather, its value is between these extreme integral values.^{2–5} A molecular model was developed from computational studies that accounts for the following experimental data: (i) the low value of the effective moment (μ_{eff}) at 300 K and its temperature dependence from 5 to 300 K and (ii) the ytterbium L_{III} -edge X-ray absorption near-edge (XANES) spectra showing the presence of f^{13} and f^{14} features that are independent of temperature from 30 to 400 K, with the f^{13} configuration dominant. A physical model, consistent with all these observations derived from CASSCF calculations, is that the ground state is an open-shell singlet consisting of $f^{13}(\pi^*)^1$ and $f^{14}(\pi^*)^0$ configurations that are lower in energy than the triplet configuration.

When the experimental studies were extended to methyl-substituted bipyridine ligands coordinated to Cp^*_2Yb , the adducts exhibited magnetic moments and n_f values that depended upon temperature, the number of methyl groups, and their positions in the bipyridine ligands (n_f accounts for f -

hole occupancy, such that when the contribution to the f^{14} configuration is 0, $n_f = 1$). The temperature dependences were fit with the Boltzmann equation and shown to result from an equilibrium between two open-shell singlet configurations. The active space in the computational model was expanded to include additional π^* configurations on the substituted bipyridine ligand, and a perturbative PT2 correction was added in order to account for these experimental results.

The studies outlined above show that the magnetic and spectroscopic properties can be described by a molecular model based upon wave function methodology. A question that naturally arises is whether the multiconfigurational ground state plays a role in the chemistry, that is, breaking and making chemical bonds, as indicated by ΔH° and ΔH^\ddagger . In this article we begin a systematic series of studies aimed at answering this question. The initial studies begin by preparing the adduct between Cp^*_2Yb and 4,5-diazafluorene (see Figure 1), which is 2,2'-bipyridine with a CH_2 group annulated in the 3,3'-position.

Special Issue: Recent Advances in Organo-f-Element Chemistry

Received: September 12, 2012

Published: November 29, 2012

This ligand may be viewed as a cyclopentadiene that shares edges with two pyridine ligands at the 1,2- and 3,4-positions. Thus, the NCCN torsion angle is fixed to be close to 0° and one of the two CH_2 hydrogens is acidic; the pK_a of CpH is 18, and that of fluorene is 22.6.⁶ The experimental and computational studies show that the ground state is multiconfigurational. The experimental studies also show that the adduct eliminates dihydrogen stoichiometrically. Combining these experimental and theoretical results allows for a molecular level of understanding of the origin of the reactivity of $\text{Cp}^*_2\text{Yb}(4,5\text{-diazafuorene})$.

EXPERIMENTAL SECTION

General Considerations. All reactions were performed using standard Schlenk-line techniques or in a drybox (MBraun). All glassware was dried at 150°C for at least 12 h prior to use. Toluene and pentane were dried over sodium and distilled, while CH_2Cl_2 was purified by passage through a column of activated alumina. Toluene- d_8 , pyridine- d_5 , and C_6D_6 were dried over sodium. All solvents were degassed prior to use. Infrared samples were prepared as Nujol mulls and taken between KBr plates and recorded on a Thermo Scientific Nicolet IS10 spectrometer. Samples for ultraviolet, visible, and near-infrared spectrometry were prepared in a Schlenk-adapted quartz cuvette, and spectra were obtained using a Varian Cary 50 scanning spectrophotometer. Melting points were determined in sealed capillaries prepared under nitrogen and are uncorrected. Elemental analyses and mass spectra (EI) were determined by the Micro-analytical Laboratory of the College of Chemistry, University of California, Berkeley, CA. X-ray structural determinations were performed at CHEXRAY, University of California, Berkeley, CA. Magnetic susceptibility measurements were made for all samples at 5 and 40 kOe in a 7 T Quantum Design Magnetic Properties Measurement System, which utilized a superconducting quantum interference device (SQUID). Sample containment and other experimental details have been described previously.⁴ The samples were prepared for X-ray absorption experiments as described previously, and the same methods were used to protect the air-sensitive compounds from oxygen and water.⁷ X-ray absorption measurements were made at the Stanford Synchrotron Radiation Lightsource on beamline 11-2. The samples were prepared and loaded into a liquid helium-flow cryostat at the beamline as described previously.⁷ Data were collected at temperatures ranging from 30 to 300 K, using a Si(220) double-crystal monochromator. Fit methods were the same as those described previously.⁷

Kinetics Experiments and NMR Experiments. ^1H NMR spectra were recorded on Bruker AVB-400 MHz, DRX-500 MHz, AV-600 MHz, and Advance 300 MHz spectrometers. ^1H chemical shifts are given relative to δ 0 (TMS). Kinetics studies were performed using a Bruker DRX-500 MHz ^1H NMR at a given temperature ($\pm 0.1^\circ\text{C}$) and by integrating data manually for each spectrum. All the data were integrated relative to an internal reference (toluene, dihydroanthracene, or the grease peak) to track mass loss during the progress of the reaction. The measured loss of intensity did not exceed 5% over the kinetic study.

Synthesis of Ligands. 4,5-Diazafuorene. The ligand 4,5-diazafuorene was prepared according to a published procedure by reducing 4,5-diazafuorenone by an excess of hydrated hydrazine ($\text{NH}_2\text{NH}_2 \cdot \text{H}_2\text{O}$; 16 h at 100°C).^{8,9} After extraction in CH_2Cl_2 , the pure 4,5-diazafuorene was sublimed at 80°C under reduced pressure. ^1H NMR (CDCl_3 , 300 K): δ (ppm) 8.78 (d, 2H, $J = 7.8$ Hz, $\text{H}_{3,6}$ or $\text{H}_{1,8}$), 7.94 (d, 2H, $J = 7.6$ Hz, $\text{H}_{1,8}$ or $\text{H}_{3,6}$), 7.35 (dd, $J = 8.0$ Hz, $\text{H}_{2,7}$), 3.92 (s, 2H, $-\text{CH}_2$). Mp: 172°C dec (lit.⁸ mp 172°C). Deuterated 4,5-diazafuorene-9,9- d_2 was prepared in a similar way using $\text{ND}_2\text{ND}_2 \cdot \text{D}_2\text{O}$ (% H $\sim 5\%$). ^1H NMR (CDCl_3 , 300 K): δ (ppm) 8.79 (d, 2H, $J = 7.6$ Hz, $\text{H}_{3,6}$ or $\text{H}_{1,8}$), 7.92 (d, 2H, $J = 8.0$ Hz, $\text{H}_{1,8}$ or $\text{H}_{3,6}$), 7.34 (2H, dd, $J = 7.8$ Hz, $\text{H}_{2,7}$), 3.92 (s, 0.08H, $-\text{CHD}$), 3.90 (s, 0.04H, $-\text{CH}_2$); 94% of the CH_2 group is deuterated. ^2D NMR (CDCl_3 , 300 K): δ 3.92 (s, CD_2).

9,9'-Bis-4,5-diaza-9H-fluorene. The ligand was prepared as described in the literature.^{10–12} Stirring 4,5-diazafuorenone for 4 h at 100°C in the presence of hydrazine hydrate gave 9,9'-bis-4,5-diaza-9H-fluorene in 45% yield. The two products (i.e., 4,5-diazafuorene and 9,9'-bis-4,5-diaza-9H-fluorene) were separated on a silica gel column (50% ethyl acetate, 50% hexane). 9,9'-Bis-4,5-diaza-9H-fluorene did not sublime but was ground into a fine powder and heated at 110°C under reduced pressure for 1 week in order to eliminate the water of hydration. ^1H NMR (CDCl_3 , 300 K): δ (ppm) 8.68 (d, 4H, $J = 4.8$ Hz), 7.31 (d, 4H, $J = 8.0$ Hz), 7.13 (dd, 4H, $J = 7.8$ Hz), 4.88 (s, 2H, $-\text{CH}$). The deuterated 9,9'-bis-4,5-diaza-9H-fluorene was prepared in a similar way using $\text{ND}_2\text{ND}_2 \cdot \text{D}_2\text{O}$ (% H $\sim 5\%$). ^1H NMR (CDCl_3 , 300 K): δ (ppm) 8.68 (d, 4H, $J = 4.8$ Hz), 7.31 (d, 4H, $J = 8.0$ Hz), 7.13 (dd, $J = 7.8$ Hz), 4.88 (s, 0.009H, $-\text{CH}$). ^2D NMR (CDCl_3 , 300 K): δ 4.92 (s, CD_2).

Synthesis of Complexes. $\text{Cp}^*_2\text{Yb}(4,5\text{-diazafuorene})$ (1). A cold toluene solution (10 mL) of $\text{Cp}^*_2\text{Yb}(\text{OEt}_2)$ (0.127 g, 0.245 mmol) was added dropwise to a cold suspension of 4,5-diazafuorene (0.042 g, 0.245 mmol) in toluene (5 mL) at 0°C . The brown-purple suspension was stirred for 2 h and then filtered at 0°C . The filtrate was cooled at -20°C , and a dark brown microcrystalline powder formed overnight (16 h). The powder was collected by filtration (101 mg, 80%), washed three times with cold toluene, and dried under reduced pressure (67 mg, 53%). ^1H NMR (toluene- d_8 , 300 K): δ (ppm) 71.07 (2H), 30.50 (2H), 6.35 (2H), 4.65 (2H), 4.23 (30H, Cp*). ^1H NMR (thf- d_8 , 297 K): δ (ppm) 45.59 (2H), 27.61 (2H), 9.51 (2H), 8.81 (2H), 3.05 (30H, Cp*). ^1H NMR (py- d_5 , 297 K): δ (ppm) 35.80 (2H), 23.41 (2H), 9.35 (2H), 6.34 (2H), 2.94 (30H, Cp*). Mp: $273\text{--}275^\circ\text{C}$. Anal. Calcd for $\text{C}_{31}\text{H}_{38}\text{N}_2\text{Yb}$: C, 60.87; H, 6.26; N, 4.58. Found: C, 60.63; H, 6.46; N, 4.45. Vis-near-IR (toluene; λ , nm (ϵ , $\text{cm}^{-1}\text{M}^{-1}$)): 474 (2840), 501 (3410), 789 (1680), 909 (2450), 1005 (1390). IR (cm^{-1}): 2962 (w), 2903 (w), 2850 (m), 1595 (w), 1578 (w), 1563 (m), 1435 (m), 1406 (s), 1378 (m), 1296 (s), 1260 (m), 1232 (m), 1164 (m), 1089 (s), 1015 (s), 924 (w), 859 (m), 796 (m), 776 (m), 765 (s), 729 (s), 695 (w). MS: $\{\text{Cp}^*_2\text{Yb}(4,5\text{-diazafuorene}) - \text{H}\} m/z$ 611.

$\text{Cp}^*_2\text{Yb}(4,5\text{-diazafuorene-}d_2)$ (1- d_2). The synthesis was similar to that used for the unlabeled compound using 145 mg (0.280 mmol) of $\text{Cp}^*_2\text{Yb}(\text{OEt}_2)$. ^1H NMR (Toluene- d_8 , 300 K): δ (ppm) 71.07 (2H), 30.50 (2H), 6.35 (2H), 4.65 (0.16H, $-\text{CH}_2$), 4.23 (30H, Cp*). ^2H NMR (C_6D_6 , 298 K): δ 4.82. Mp: $273\text{--}275^\circ\text{C}$. Anal. Calcd for $\text{C}_{31}\text{H}_{36}\text{D}_2\text{N}_2\text{Yb}$: C, 60.67; H, 5.95; N, 4.59. Found: C, 59.56; H, 6.07; N, 4.31. Vis-near-IR (toluene, λ , nm (ϵ , $\text{cm}^{-1}\text{M}^{-1}$)): 474 (2840), 501 (3410), 789 (1680), 909 (2450), 1005 (1390). IR (cm^{-1}): 2183 (m), 2117 (w), 1580 (m), 1538 (m), 1459 (m), 1396 (s), 1378 (m), 1292 (s), 1260 (m), 1246 (m), 1163 (s), 1095 (s), 1015 (s), 934 (w), 799 (m), 757 (m), 731 (s). MS: $\{\text{Cp}^*_2\text{Yb}(4,5\text{-diazafuorene-}d_2) - \text{D}\} m/z$ 612.

$\text{Cp}^*_2\text{Yb}(4,5\text{-diazafuorenyl})$ (2). The complex $\text{Cp}^*_2\text{Yb}(\text{OEt}_2)$ (0.127 g, 0.245 mmol) was mixed with 4,5-diazafuorene (0.042 g, 0.245 mmol), and toluene (10 mL) was added at room temperature. The brown-purple suspension was stirred for 48 h at 70°C , cooled to room temperature, and filtered. The volume of the filtrate was reduced to 2 mL, and the deep purple solution was cooled at -20°C . The small dark purple crystals that formed were collected by filtration and dried under reduced pressure (77 mg, 52%). ^1H NMR (toluene- d_8 , 300 K): δ (ppm) 122.19 (2H), 31.54 (2H), 16.78 (2H), 11.83 (1H), 3.69 (30H, Cp*) ^1H NMR (thf- d_8 , 297 K): δ (ppm) 123.51 (2H), 31.94 (2H), 16.85 (2H), 11.57 (1H), 3.66 (30H, Cp*). ^1H NMR (py- d_5 , 297 K): δ (ppm) 124.38 (2H), 32.32 (2H), 17.16 (2H), 12.02 (1H), 3.98 (30H, Cp*). Mp: $275\text{--}278^\circ\text{C}$ dec. Anal. Calcd for $\text{C}_{31}\text{H}_{37}\text{N}_2\text{Yb}$: C, 60.97; H, 6.11; N, 4.59. Found: C, 61.04; H, 5.94; N, 4.48. Vis-near-IR (λ , nm (ϵ , $\text{cm}^{-1}\text{M}^{-1}$)): 426 (1250), 502 (360), 538 (405), 581 (395), 634 (210), 963 (40), 908 (30), 1001 (55). IR (cm^{-1}): 2954 (w), 2924 (w), 2854 (m), 2725 (m), 1561 (m), 1528 (w), 1460 (s), 1408 (w), 1377 (s), 1327 (w), 1300 (m), 1261 (m), 1260 (m), 1164 (w), 1090 (s), 1020 (s), 947 (w), 888 (w), 798 (s), 781 (m), 726 (m), 684 (m).

$\text{Cp}^*_2\text{Yb}(4,5\text{-diazafuorenyl-}d)$ (2- d). The synthesis was similar to that used for the unlabeled complex from 51 mg (0.099 mmol) of

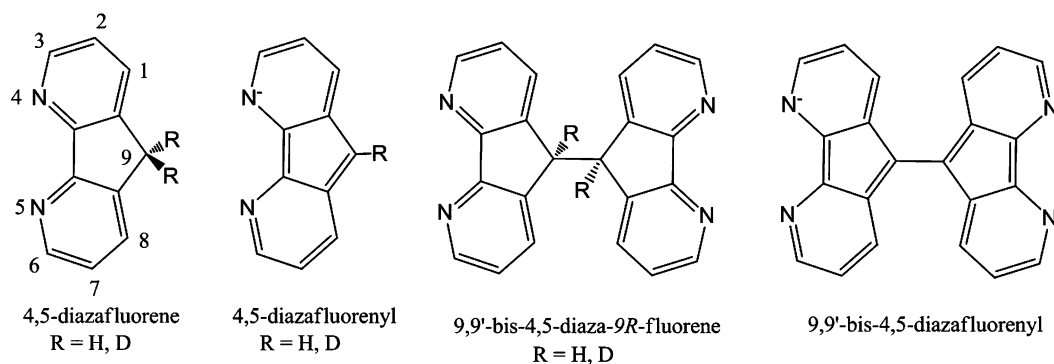


Figure 1. Numbering scheme and names of the ligands used in this work.

Table 1. Solid-State Properties of Complexes 1–4

compd	color	mp (°C)	IR (cm ⁻¹)	$\chi T(300\text{ K})$	$\mu_{\text{eff}}(300\text{ K}) (\mu_{\text{B}})$
Cp* ₂ Yb(4,5-diazafluorene) (1)	dark green	273–275	2923, 2900	0.15	1.1
Cp* ₂ Yb(4,5-diazafluorenyl) (2)	dark red	275–278	3044, 3009	2.55	4.52
Cp* ₂ Yb(4,5-diazafluorene-d ₂) (1-d ₂)	dark green	273–275	2183, 2117	0.17	1.2
Cp* ₂ Yb(4,5-diazafluorenyl-d) (2-d)	dark red	275–276	2360, 2342	2.54	4.51
(Cp* ₂ Yb) ₂ (9,9'-bis-4,5-diazafluorene) (3/3-d ₂) ^a	dark brown			0.31	1.6
(Cp* ₂ Yb) ₂ (9,9'-bis-4,5-diazafluorenyl) (4) ^b	deep purple				

^aObtained as a powder. ^bIsolated product.

Cp*₂Yb(OEt)₂. Mp: 275–276 °C dec. IR (cm⁻¹): 2923 (s), 2854 (s), 2360 (m), 2342 (m), 1529 (w), 1518 (w), 1463 (s), 1377 (m), 1328 (w), 1319 (w), 1309 (w), 1261 (m), 1204 (m), 1091 (m), 1018 (m), 799 (s), 780 (m), 737 (w), 724 (m), 668 (w). ²H NMR (toluene-d₈, 297 K): δ (ppm) 11.98.

In Situ Synthesis of (Cp*₂Yb)₂(9,9'-bis-4,5-diazafluorene-d₂) (3/3-d₂). A 1:1 brown mixture of 9,9'-bis-4,5-diazafluorene-d₂ and Cp*₂Yb(OEt)₂ in C₆D₆ was stirred vigorously for 30 s and then transferred quickly into a NMR tube adapted with a J. Young valve and quickly cooled in liquid N₂ (77 K) once outside the drybox. The sample was transported to the NMR spectrometer, rapidly warmed to room temperature, and then inserted into the probe, precooled at a given temperature. The kinetics data were collected from 290 to 315 K over at least 3 half-times. ¹H NMR (C₆D₆, 300 K): δ (ppm) 79.20 (4H), 25.08 (4H), -0.591 (4H), 5.40 (30H, Cp*), 3.84 (30H, Cp*). The kinetics were also obtained at room temperature using an analogous procedure but followed by visible spectroscopy for the labeled and unlabeled complexes.

Isolation of (Cp*₂Yb)₂(9,9'-bis-4,5-diazafluorenyl) (4). A cold diethyl ether solution of Cp*₂Yb(OEt)₂ was added to an ether suspension of 9,9'-bis-4,5-diazafluorene at -77 °C. The brown solution that formed was stirred at -77 °C for 5 h, warmed to -40 °C, and stored for 2 days at -40 °C and 5 days at -20 °C. The brown-purple solution was then stirred at 0 °C for 12 h and at room temperature for another 12 h. Solvent was removed under reduced pressure, and the brown residue was analyzed by ¹H NMR spectroscopy. Two sets of signals in a 1:1 ratio were observed. The two products were identified as complexes 2 and 4. Complex 4 was identified only by X-ray crystallography, since only a small amount was obtained. The purple X-ray-suitable crystals were obtained by cooling a concentrated (30 mM) solution to 10 °C.

X-ray Crystallography. Single crystals of compounds 2 and 4 were coated in Paratone-N oil and mounted on a Kapton loop. The loop was transferred to either a Bruker SMART 1000 or SMART APEX diffractometer equipped with a CCD area detector. Preliminary orientation matrixes and cell constants were determined by collection of 10 s frames, followed by spot integration and least-squares refinement. Data were integrated by the program SAINT and corrected for Lorentz and polarization effects. Data were analyzed for agreement and possible absorption using XPREP. A semiempirical, multiscan absorption correction was applied using SADABS. This

model corrects the absorption surface using a spherical harmonic series based on differences between equivalent reflections. The structures were solved by direct methods using SHELX. Non-hydrogen atoms were refined anisotropically, and hydrogen atoms were placed in calculated positions and not refined for 4, but their positions were refined for 2.

RESULTS AND DISCUSSION

The results are presented in five separate sections: (i) synthesis and general characterization; (ii) solution mechanistic studies of the thermal elimination of dihydrogen as 1 (Cp*₂Yb(4,5-diazafluorene)) goes to 2 (Cp*₂Yb(4,5-diazafluorenyl)); (iii) electronic structural studies of 1; (iv) computational results; (v) a general discussion that presents our molecular level of understanding of the origin of the reactivity of 1.

Synthesis and Characterization. The complex Cp*₂Yb(4,5-diazafluorene) (1; see Figure 1 for the structural formulas and numbering system for the ligands used in this article) is prepared by mixing a cold (0 °C) toluene solution of Cp*₂Yb(OEt)₂ with a cold (0 °C) toluene suspension of 4,5-diazafluorene. The resulting brown powder sublimates as dark green crystals at 190 °C at 10⁻² mm, gives a M - 1⁺ molecular ion in the mass spectrum, and melts at 273–275 °C. Attempts to grow crystals from solution were unsuccessful, and those obtained from sublimation were not suitable for an X-ray diffraction study. The temperature (0 °C) for the synthesis is important, since reactions carried out at room temperature give ¹H NMR spectra that contain resonances due to several metallocene compounds. In the 0 °C temperature synthesis, the resulting ¹H NMR spectrum is, however, largely free of these additional resonances.

In order to examine the origin of the temperature effect on the synthesis, the ¹H NMR spectrum in C₆D₆ was monitored at 60 °C over time at millimolar concentration. The resonances due to 1 convert into a major product with a 90% conversion after 2 days. The product is shown to be the complex Cp*₂Yb(4,5-diazafluorenyl) (2) by heating 1 in toluene at 70

°C for 2 days. Crystallization from toluene gave **2** as dark red crystals in moderate yield. Some physical properties of **1** and **2** and their deuterio derivatives are given in Table 1. Compound **2** is derived from **1** by the loss of a hydrogen atom; when the reaction is monitored by NMR spectroscopy, H₂ is detected.

An ORTEP of **2** is shown in Figure 2; crystal data and packing diagrams are available in the Supporting Information.

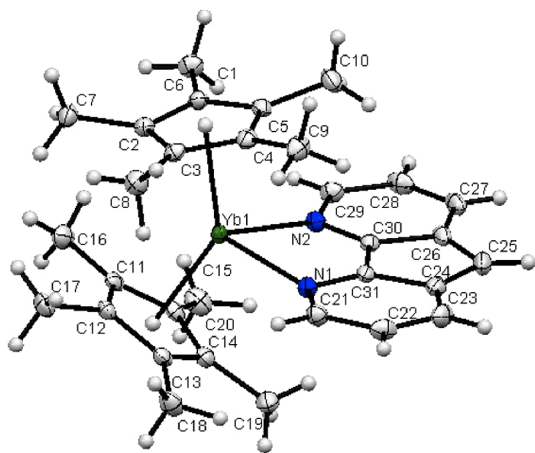
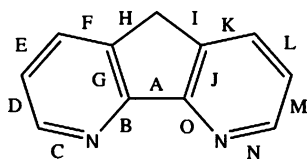


Figure 2. ORTEP for Cp*₂Yb(4,5-diazafluorenyl) (**2**). Ellipsoids are given at the 50% probability level, the non-hydrogen atoms are refined anisotropically, and the hydrogen atoms are refined isotropically.

Table 2. Selected Bond Distances (Å) and Angles (deg) for Cp*₂Yb(4,5-diazafluorenyl) (**2**)



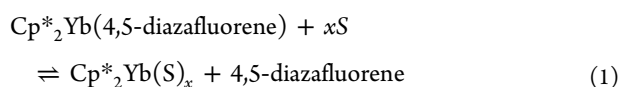
bond	
A	1.414(3)
B, O, av	1.354(1)
C, N, av	1.338(1)
D, M, av	1.403(1)
E, L, av	1.375(1)
F, K, av	1.398(1)
G, J, av	1.445(3)
H, I, av	1.419(1)
bond or angle	
Yb–C (distance range)	2.599(2)–2.632(2)
Yb–C (ring), av	2.609 ± 0.009
Yb–Cp (cent), av	2.31
Cp (cent)–Yb–Cp (cent)	140
Yb–N, av	2.372 ± 0.001
torsion angle N–C–C–N	0.5
torsion angle C–C–C–C	0.7

Some selected bond lengths and angles are given in Table 2. Four features of the solid-state structure are important relative to the electronic structure. (i) Only one hydrogen atom is attached to C(25), which is located and refined isotropically. The angles C(24)–C(25)–H and C(26)–C(25)–H are 124(2) and 128(2)°, respectively, and since the C(24)–

C(25)–C(26) angle is 107.7(2)°, the geometry at C(25) is trigonal planar. (ii) The C(24)–C(25) and C(25)–C(26) distances are 1.421(3) and 1.417(3) Å, respectively, in the range found for C(sp₂)–C(sp₂) distances in nonfused heterocycles of 1.41–1.43 Å.¹³ (iii) The average Yb–C(Cp) distance of 2.609 ± 0.009 Å is close to the Yb^{III}–C(Cp) distance of 2.59 ± 0.01 Å in [Cp*₂Yb(bipy)]⁺[Cp*₂YbCl₂]^{–14} and significantly shorter than the Yb^{II}–C distance of 2.74 ± 0.04 Å in Cp*₂Yb(py)₂.¹⁵ (iv) The average Yb–N distance of 2.372 ± 0.001 Å is identical with the Yb^{III}–N distance in [Cp*₂Yb(bipy)]⁺[Cp*₂YbCl₂]^{–14} of 2.372 ± 0.005 Å and significantly shorter than the Yb^{II}–N distance of 2.565 ± 0.010 Å in Cp*₂Yb(py)₄.¹⁵ These bond lengths and angles in **2** are in agreement with a Cp*₂Yb fragment based upon Yb(III) and a diazafluorenyl fragment that carries a negative charge. Accordingly, the Yb in **2** is f¹³, which implies that Yb is f¹⁴ in **1**, since **1** and **2** differ by a single hydrogen atom.

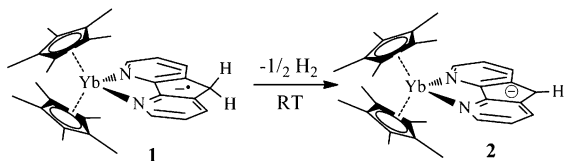
Although **1** and **2** differ by one hydrogen, their ¹H NMR spectra show that both are paramagnetic compounds; the chemical shifts at 25 °C are given in the Experimental Section. The variable-temperature ¹H NMR chemical shifts for **2** shown as a δ vs 1/T plot (Supporting Information, Figure S1) are linear in temperature and therefore follow Curie behavior. This behavior is expected for an isolated Yb(III) paramagnet and consistent with the formulation deduced from the X-ray structure: viz., Cp*₂Yb^{III}(4,5-diazafluorenyl). Although the ¹H NMR chemical shifts of **1** are indicative of a paramagnetic molecule, a plot of δ vs 1/T shows that all of the resonances except those due to Cp* are decidedly nonlinear (Supporting Information, Figure S2). The nonlinear behavior is reminiscent of the resonances observed for Cp*₂Yb(bipy) and its substituted derivatives.^{1–4,7,14} The nonlinearity is the first clue that the electronic structure of **1** is based upon intermediate-valent ytterbium, rather than divalent ytterbium, a point developed below.

Another notable difference between the ¹H NMR spectra of **1** and **2** is the different solvent dependence of their chemical shifts at 25 °C; the resonances of **1** depend strongly upon the solvent, while those of **2** do not. Thus, the most deshielded resonance, due to 2H's in **1** in toluene-*d*₈, is a singlet at 71.1 ppm that moves upfield to 45.6 or 35.8 ppm in either thf-*d*₈ or pyridine-*d*₅, respectively. The other resonances due to the diazafluorene ligand shift slightly (±3–4 ppm), and those due to the Cp* resonances are shielded by about 1 ppm in either thf-*d*₈ or pyridine-*d*₅; the values are given in the Experimental Section. Although the resonance at δ 71.1 ppm in toluene-*d*₈ is not assigned with certainty, it is likely due to the CH that is α to N, since these resonances are the most strongly deshielded in the bipy adducts due to their proximity to the paramagnetic center, giving rise to a large dipolar contribution to the total chemical shift tensor.^{1,2} A possible interpretation of these solvent effects is the equilibrium shown in eq 1. Synthetic support for this postulate is obtained by heating **1** in pyridine-*d*₅ for several days at 60 °C in an NMR tube. The resulting material has NMR resonances due to Cp*₂Yb(py)₂ and free diazafluorene. Since the pyridine adduct is diamagnetic and **1** is paramagnetic, the equilibrium illustrated in eq 1 implies a reversible electron transfer. A similar equilibration between Cp*₂Yb(bipy) and 4,4'-Me₂bipy and related adducts was noted previously.^{4,14}



Mechanism Studies. The mechanism of dihydrogen elimination in the thermal rearrangement of **1** to **2** (Scheme 1) is not obvious but is of considerable interest.

Scheme 1



Since the reaction is relatively clean but slow at 20 °C, according to the NMR spectra, the time evolution was studied by observing the ¹H NMR and vis–near-IR spectra. In C₆D₆, the spectral intensity of **1** was estimated by the total numbers of hydrogens in **1** and their decrease with time is illustrated in the Supporting Information, together with a plot of ln(*C*/*C*₀) as a function of time, where *C* is the concentration of **1**. The total number of hydrogens is used, rather than just using the Cp* resonances, because the Cp* resonances of **1** and **2** overlap at some temperatures. These plots are nonlinear and cannot be used to extract a rate law with confidence over the course of the reaction; these are available (Figures S3 and S4 in the Supporting Information). Hence, the values of *t*_{1/2} for the reaction were estimated by determining the time at which the concentration of **1-h**₂ equals that of **2-h** and the values of *t*_{1/2} for **1-d**₂ yielding **2-d** were determined similarly. Over the temperature range of 20–87 °C, the values of *t*_{1/2}(h)/*t*_{1/2}(d) vary from 6.4 to 6.2. These rather large values show that breaking the C–H or C–D bond occurs before or during the slow step or steps in the reaction. In addition, the *t*_{1/2} values are used to determine the influence of added H₂ or D₂ on the overall rate. Since the vis–near-IR spectrum of **1-h**₂ has a feature at 909 nm that does not appear in **2-h**, this absorption was monitored as a qualitative indicator of the reaction rate. Since the concentration of starting material is an order of magnitude lower in the vis–near-IR spectrum, the rate is correspondingly slower. As the reaction rate is much slower, typically days (vis–near-IR) rather than minutes (NMR) at 20 °C, the reaction was studied over the first 10% of the reaction, using the method of initial rates. The values of *k*_{obs}(H) and *k*_{obs}(D) at 60 °C are available (Figure S5 in the Supporting Information). The *k*_{obs}(H)/*k*_{obs}(D) value of 6.8 is in agreement with values obtained from the NMR spectra. Since these rate data are qualitative, additional studies were performed to gain additional information about the mechanism.

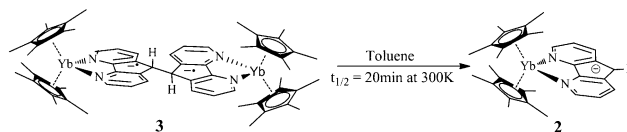
The rate of rearrangement of **1-h**₂ to **2-h** was followed under an atmosphere of N₂ and then compared to the rate under 1 atm of H₂ or D₂. In each case, the rates were unchanged when followed by NMR spectroscopy. However, under D₂, HD is observed in the spectrum, but when isolated **2** is exposed to an atmosphere of D₂ in an NMR tube, no HD is observed and no deuterium is incorporated into **2**. The rearrangement was monitored in the presence of dihydroanthracene or 1,4-cyclohexadiene as potential radical traps. In each case no resonances due to anthracene or benzene were observed, and the rates were qualitatively similar to those observed in the absence of the traps. As the rate of the reaction shows strong

concentration dependence, the reaction is not a unimolecular decomposition. A crossover experiment was studied by mixing equimolar amounts of **1-h**₂ and **1-d**₂ in C₆D₆; following the reaction at 60 °C shows that H₂ and HD are both formed, but the amount of H₂ is greater than that of HD, as a result of the primary isotope effect. The formation of HD is consistent with crossover and a bimolecular process.

At this point in the mechanistic study, the deductions are that the rate of the reaction (i) depends upon concentration of **1**, (ii) has a large primary isotope effect, (iii) free radicals are not involved, (iv) neither H₂ nor D₂ influences the rate but HD is formed under a D₂ atmosphere and HD and H₂ are formed in a crossover experiment.

The next kinetic study, however, is crucial in the evolution of a proposed mechanism for the reaction. In a NMR tube, the C–C-bonded dimer, 9,9'-bis-4,5-diaza-9H-fluorene (see Figure 1 for a drawing) was mixed with Cp*₂Yb(OEt)₂ in C₆D₆ at room temperature. Examination of the ¹H NMR spectrum within minutes showed that **2-h** was formed cleanly (Scheme 2). A similar reaction was observed when the deuterated analogue was used.

Scheme 2



Since this reaction is clean and rapid, the disappearance of the two farthest downfield resonances was monitored in the NMR spectrum from 17 to 42 °C over 3 half-lives. The ln(*C*/*C*₀) plots as a function of time are linear and yield a first-order rate constant, *k*_H, of 1.10 × 10^{−3} s^{−1} at 27 °C. Similarly, the value of *k*_D at 27 °C is 1.00 × 10^{−3} s^{−1}. Plots of these data are available in the Supporting Information. The *k*_H/*k*_D value is 1.1, showing that the cleavage of the C–C bond does not involve C–H bond cleavage before the slow step. The rate of the reaction as a function of temperature gives Δ*H*[‡] = 23(1) kcal mol^{−1} and Δ*S*[‡] = 3(1) cal mol^{−1} K^{−1}. The Eyring plot is shown in Figure 3. When **3** is allowed to rearrange to **2** under an atmosphere of D₂, no HD is observed in the ¹H NMR spectrum.

The concentration dependence of the rate of reaction of **3** to **2** was also followed by vis–near-IR spectroscopy, since the concentration is an order of magnitude less than that in the NMR experiment. The plot of ln(*C*/*C*₀) against time was

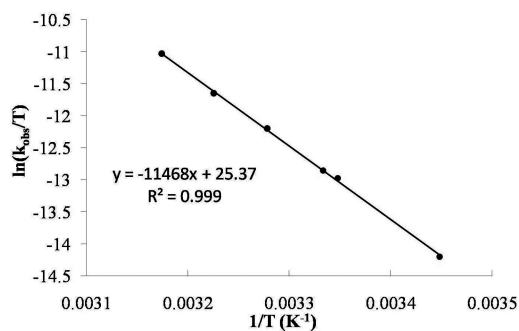


Figure 3. Eyring plot for the complex [(Cp*₂Yb)₂(9,9'-bis-4,5-diaza-9D-fluorene)] (**3-d**₂) going to Cp*₂Yb(4,5-diazafluorenyl-d) (**2-d**).

obtained over 3 half-lives, and the k_H value was $0.6 \times 10^{-3} \text{ s}^{-1}$ at 20 °C. The near equality of the rates determined in the vis–near-IR and NMR experiments shows that the reaction does follow a first-order rate law, and the low value of the entropy of activation is consistent with the notion that the C–C bond cleavage step occurs after the transition state. The fact that the rate of reaction of 3 to 2 is much faster than the rate of reaction of 1 to 2 is consistent with the intermediate formation of 3 from 1, implying the sequence of elementary reactions as 1 → 3 → 2. This idea is outlined in more detail in the Discussion.

In the process of collecting the data for the Eyring plot for the reaction of 3 to 2 (Figure 3), resonances of another compound were detected in the ^1H NMR spectrum in the reactions at temperatures below 27 °C. On a synthetic scale, when 9,9'-bis-4,5-diaza-9H-fluorene is mixed with $\text{Cp}^*_2\text{Yb}(\text{OEt}_2)$ in Et_2O at –78 °C and the mixture is warmed slowly to 0 °C over approximately 2 weeks, a brown powder identified as 2 by NMR spectroscopy was obtained that contained purple crystals of a compound identified as 4 by X-ray crystallography. The ORTEP (Figure 4) shows that 4 is 9,9'-bis-4,5-

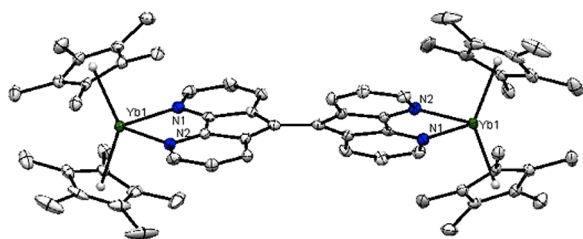


Figure 4. ORTEP drawing of complex 4. The hydrogens and the cocrystallized solvent molecule are removed for clarity.

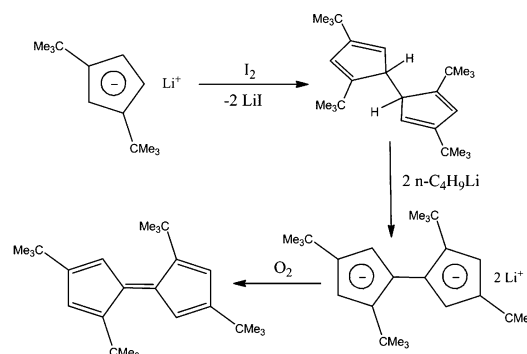
diazafluorenylidene coordinated to two Cp^*_2Yb fragments. The Yb–C(Cp^*) and Yb–N distances are in the range found for Yb(III). The two carbene fragments are linked by a C–C double bond of 1.463(9) Å with a torsion angle between the two fragments of 39°. In the free ligand the C–C distance is 1.385(4) Å and the torsion angle is 38°. The C–C bond in 4 is therefore a stretched double bond and the complex is chiral with C_2 symmetry.

Although the resonances in the NMR spectra due to 3 and 4 are absent during the transformation of 1 to 2 at temperatures greater than 27 °C, those due to 4 are observed at lower temperature. Once isolated, 4 is stable at room temperature, which implies that the rate of the transformation of 3 to 2 is faster than that of 3 to 4 and 4 is not on the pathway from 3 to 2 and therefore is not the source of dihydrogen. The identity of 4 also is consistent with the postulate that 3 is the 2:1 adduct as shown in Scheme 2.

The conversion of the diazafluorene adduct 3 to 4 is, in a sense, related to the conversion of the isomers of $(\text{Me}_3\text{C})_2\text{C}_3\text{H}_4$ to dihydrofulvalene and then to fulvalene (Scheme 3).¹⁶ The analogy between the conversion of CpH or the 3,3'- CH_2 annulated to bipyridine is invoked later when the reaction mechanism is discussed.

Two studies involving formation of H_2 from 4,5-diazafluorene coordinated to d transition metals are relevant to the studies outlined above. Mach and co-workers observed dihydrogen evolution when 4,5-diazafluorene was added to $\text{Cp}'_2\text{Ti}(\text{Me}_3\text{SiCCSiMe}_3)$ ($\text{Cp}' = \text{C}_5\text{H}_5, \text{C}_5\text{HMe}_4, \text{C}_5\text{Me}_5$), and they isolated the $\text{Cp}'_2\text{Ti}^{\text{III}}(4,5\text{-diazafluorenyl})$ adduct.¹⁷ Song and co-workers reported that $\text{Ru}(\text{PPh}_3)_2(\text{H}_2)(4,5\text{-diazafluor-}$

Scheme 3



ene) and $\text{Ru}(\text{PPh}_3)_2(\text{H})(\text{N}_2)(4,5\text{-diazafluorenyl})$ can be interconverted by N_2 and H_2 .¹⁸

Electronic Structure. The solid-state magnetism of 1, 1- d_2 , 2, and 2- d was studied over the temperature range 2–360 K, and plots are shown in Figure 5 and in Figure S13 (Supporting

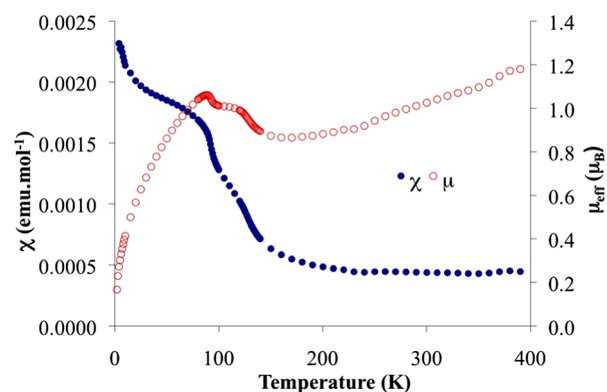


Figure 5. Plots of μ_{eff} and χ vs T (K) for the complex $\text{Cp}^*_2\text{Yb}(4,5\text{-diazafluorene})$ (1) in the temperature range 2–300 K.

Information). Complex 1 exhibits a low magnetic moment, $\mu_{\text{eff}} = 1.2 \mu_B$ at 360 K, as observed for the decamethylterbocene adducts with various bipyridine ligands.^{1–4,7} As in these adducts, when 4,5-diazafluorene is reduced by the Yb(II) center, a hole is created in the Yb(III) center (f^{13}) as the electron enters the π^* orbital of the ligand, and the calculated effective moment for the complex is expected to be $4.8 \mu_B$ at 300 K if the spins are uncorrelated ($^2F_{7/2} + ^2S$).

The low effective moment observed for complex 1 clearly implies that the two spins are correlated. However, this information is not sufficient to allow a quantitative description of its electronic structure. Inspection of the χ vs T plot indicates that the correlation is not straightforward, since a plateau is observed in the temperature range 150–300 K (Figure 5). Moreover, the very low magnetic moment observed in 1 makes these data susceptible to so-called “Curie tails” from trace amounts of magnetic impurities, such as $J = 7/2$ impurities. The data in Figure 5 were obtained on a sample that was sublimed and therefore highly pure material results in two discontinuities occurring at 83 and 120 K. Thus, the temperature-dependent magnetic data of 1 show a very low magnetic susceptibility and temperature-independent paramagnetic (TIP) behavior in the high-temperature regime as well as a low-temperature regime with two distinct transitions between these regimes. In earlier

studies, a molecular model was developed from CASSCF calculational studies that traced the temperature-dependent magnetic and XANES behavior to one or two open-shell singlet states that lie below the triplet state. If the two open-shell singlet states are close in energy, their population change as a function of temperature can be modeled by a Boltzmann distribution between these two singlet states, referred to as SS1 and SS2. The TIP behavior is thought to result from van Vleck mixing of triplet character into the singlet states. The experimental magnetic and spectroscopic data for $\text{Cp}^*_2\text{Yb}(4,5\text{-diazafuorene})$ (**1**) are treated in an analogous way as outlined below.

The Yb L_{III} -edge XANES spectra were recorded at different temperatures over a 30–300 K range (Figure 6). At room

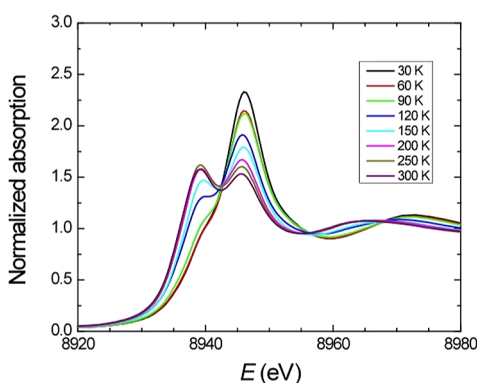


Figure 6. Yb L_{III} -edge XANES data for the complex $\text{Cp}^*_2\text{Yb}(4,5\text{-diazafuorene})$ (**1**) at various temperatures.

temperature, two white line features are visible, in agreement with the presence of both f^{14} and f^{13} character for complex **1** in a 0.62:0.38 ratio. The f^{14} feature decreases while the f^{13} feature increases with decreasing temperature. The magnetic susceptibility data indicated the presence of TIP behavior at lower temperature. It is possible to rationalize TIP behavior with the presence of a hole on the Cp^*_2Yb fragment and an electron in the ligand that results in the formation of an open-shell singlet that is lower in energy than the triplet. The electron that is transferred to the ligand has several accessible π^* orbitals, resulting in several possible open-shell singlets of different configurations that are lower in energy than that of the triplet. Each of the open-shell singlets has different magnetic properties because of the relative amount of the π^* contribution to the configurations of the $f^{13}\text{-}\pi^{*1}$ states in comparison to the f^{14} configuration, which is diamagnetic ($\chi < 0$). In the magnetic data for **1** (Figure 5) two transitions are observed at 83 and 120 K. From these data, it is possible to rationalize the presence of three possible open-shell singlet states (SS) below the triplet that have comparable energies and are thermally populated as the temperature increases, leading to the observation of the two transitions $\text{SS1} \leftrightarrow \text{SS2}$ and $\text{SS2} \leftrightarrow \text{SS3}$. However, the Boltzmann fits only used two singlet states below the triplet because the valence change between SS1 and SS2 is likely too subtle to be detected by the n_f results, which are only precise to a few percent. The enthalpy and entropy changes determined from the Boltzmann fits to these XANES results are in reasonable agreement with those obtained by similar fits to the magnetic data and are given in the captions of Figures 7 and 8 and are discussed in the Discussion.

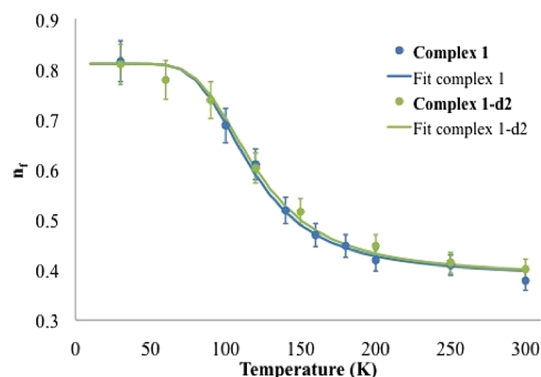


Figure 7. Plot of n_f vs T (K) for the complex $\text{Cp}^*_2\text{Yb}(4,5\text{-diazafuorene})$ (**1**) and **1-d2**. The best fits are obtained from a Boltzmann distribution between two singlet states using the following parameters: (**1**) $n_{f1} = 0.81$, $n_{f2} = 0.38$, $\Delta H = 5.1(3)$ kJ mol $^{-1}$, $\Delta S = 43(5)$ J mol $^{-1}$ K $^{-1}$; (**1-d2**) $n_{f1} = 0.81$, $n_{f2} = 0.38$, $\Delta H = 5.1(3)$ kJ mol $^{-1}$, $\Delta S = 42(5)$ J mol $^{-1}$ K $^{-1}$.

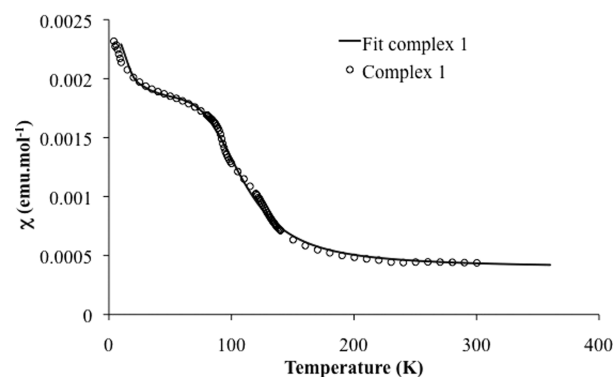


Figure 8. Plots of μ_{eff} and χ vs T (K) for the complex $\text{Cp}^*_2\text{Yb}(4,5\text{-diazafuorene})$ (**1**). The best fit is obtained from a Boltzmann distribution between two singlet states using the following parameters: $\chi_{\text{SS1}} = 0.00174$ emu mol $^{-1}$, $\chi_{\text{SS2}} = 0.00038$ emu mol $^{-1}$, $\Delta H = 5.27(5)$ kJ mol $^{-1}$, $\Delta S = 47.5(2)$ J mol $^{-1}$ K $^{-1}$, $C_{\text{imp}}/T = 0.00055$ emu mol $^{-1}$ K $^{-1}$.

For complex **2**, both the magnetism in the 2–300 K temperature range and the Yb L_{III} XANES measurements at room temperature as well as at 30 K are in agreement that this complex is an isolated f^{13} paramagnet, $\text{Cp}^*_2\text{Yb}^{\text{III}}(\text{fluorenyl})$, and implies that the negative charge is delocalized on the fluorenyl ligand as deduced above.

The vis–near-IR spectra were recorded for **1**, **2** and **3** in toluene in the 300–1100 nm wavelength range and are shown in the Supporting Information. The spectra of **1** and **3** are very similar and present a very broad and intense band in the vis–near-IR region (700–1100 nm), which is attributed to $\pi^* \rightarrow \pi^*$ transitions, since the spectral profile is very similar to those of both $\text{Cp}^*_2\text{Yb}(\text{bipy})$ and $\text{Na}(\text{bipy})$.^{5,14} This band has a maximum at 909 nm. On the other hand, the spectrum from **2** displays only a set of three low-intensity, yet relatively sharp, bands in the range characteristic of $f^{13} f \rightarrow f$ transitions.^{5,14,19} The disappearance of the band with a maximum at 909 nm was used to follow the time dependence and therefore the rate of reaction because it is a signature of the presence of unpaired spin density in the ligand in **1** and **3** and is situated in the range in which **2** does not absorb.

Calculations. In order to gain insight into the electronic structure of **1**, computational investigations were carried out

using the methodology described in previous studies.^{1,7} Geometry optimizations were carried out using f-in-core RECP (adapted to the +II and +III oxidation states) at the DFT level (B3PW91). The structure obtained with a +III oxidation state RECP is in agreement with the X-ray structure of **2**, shown in Figure 2 (bond A is 1.413 Å and the Yb–N distance is 2.396 Å). The structural parameters obtained for **2** were used in the CASSCF calculations for **1**. As reported in the bipyridine systems,^{1,7} a CAS definition of 4 active orbitals (2f and the 2 lowest π^*) and 4 active electrons leads to similar results as a bigger CAS with 8 active orbitals (6f and 2 π^*) and 12 active electrons, so that the former was used. State-specific calculations were carried out for the three lowest singlets and the lowest triplet. The lowest electronic state is predicted to be an open-shell singlet with a mixture of 84% $f^{13}(\pi^*)^1$ and 16% f^{14} in which π^* is composed of 55% of π^*_1 and 45% of π^*_2 . A second open-shell singlet is found 0.24 eV higher in energy and is also a mixture of 39% $f^{13}(\pi^*)^1$ and 61% f^{14} in which π^* is composed of 74% of π^*_1 and 26% of π^*_2 . The closed-shell singlet is found 2.38 eV higher in energy. The lowest triplet is predicted to be 0.55 eV above the lowest singlet and is based on a pure $f^{13}\pi^*_1$ configuration. Despite our considerable effort, it is not possible to locate a third singlet state lower than the triplet. These computational results (Figure 9 and Table 3) are in accord with the experimental observations for **1**.

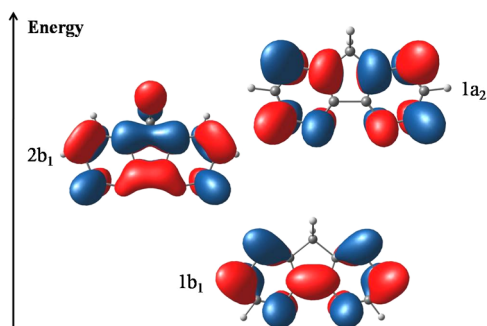


Figure 9. Representation (extended Hückel calculation) of the three lowest π^* orbitals of 4,5-diazafluorene, their relative energies and corresponding labels in C_{2v} symmetry.

Table 3. State Configuration Fractions for f orbitals and π^* Orbitals As Calculated by CASSCF

label	f^{13}	f^{14}	n_f
SS1	0.84	0.16	0.84
SS2	0.39	0.61	0.39
configuration	π^*_1	π^*_2	
SS1	0.55	0.45	
SS2	0.74	0.26	

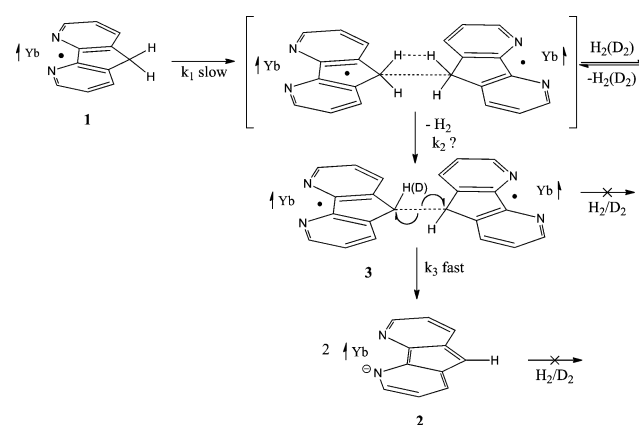
DISCUSSION

The interpretation of the experimental studies outlined above is that the ytterbium complex **1** has an intermediate valence between +II and +III, while the valence in **2** is +III. Compound **2** is therefore an isolated paramagnet based upon a $2J_{7/2}$ state but **1** is multiconfigurational, like the $Cp^*_2Yb(\text{bipyridine})$ adducts reported earlier. The experimental results for **1** show that at least two open-shell singlet states are lower in energy than the triplet state and there is an equilibrium between the two low-lying open-shell singlet states, SS1 and SS2. The

thermochemical quantities ΔH and ΔS are obtained for the equilibrium $SS1 \rightleftharpoons SS2$ by fitting the Boltzmann distribution to the values of χ and n_f obtained as a function of temperature. The values of ΔH and ΔS show that SS1 is favored by enthalpy and SS2 is favored by entropy; at 300 K, SS2 is favored by about -8 kJ/mol over SS1. A similar thermochemical result is observed for the methyl-substituted bipyridine adducts. Since CASSCF calculations indicate that the SS1 has an n_f value of 0.84, Yb(III) dominates Yb(II), consistent with shorter Yb–C(Cp^*) and Yb–N bonds in the former adducts. In SS2, the contribution is inverted and the longer Yb–C(Cp^*) and Yb–N bonds result in an increase in entropy. The computational results provide a molecular level of understanding of the thermochemistry. Although the 4,5-diazafluorene and bipyridine adducts of Cp^*_2Yb have multiconfigurational ground states, they differ in their reactivity; **1** eliminates H_2 , whereas the bipy adducts are thermally stable.

A possible mechanism that is consistent with the experimental facts for the transformation of **1** to **2** by way of **3** is outlined in Scheme 4. Adduct **1** has biradical character, and

Scheme 4



the 4,5-diazafluorene ligand has unpaired spin density distributed in various p_π orbitals located on the nitrogen and carbon atoms. Since the LUMO+1 of 2b₁ symmetry has unpaired spin density at C(9), the p orbital on C(9) is presumably the “active orbital” that is the trigger for chemistry at C(9). If this conjecture is correct, the unpaired spin density at C(9) initiates cleavage of a C–H bond, resulting in formation of H_2 and a C–C bond at C(9) in **3**. The mechanism of this step is not clear, but the experimental studies show that a bimolecular process is involved. A possible transition state is shown in brackets, in which H_2 is eliminated heterolytically as the C–C bond forms. This step may account for the HD formation in the crossover experiment.²⁰ If this step (k_2) is slow, then the rate will show a concentration dependence. Since **3** can be generated and is shown to rearrange rapidly to **2**, k_3 is faster than either k_1 or k_2 . The step involving k_3 is homolytic cleavage of the C–C bond that results in formation of the 4,5-diazafluorenyl adduct **2** or H_2 elimination forming **4**, depending upon the temperature. The k_2 step is reminiscent of the dimerization of a cyclopentadiene to dihydrofulvalene and then to fulvalene,²¹ as in Scheme 3.¹⁶ In the reaction shown in Schemes 3 and 4, the important step in coupling two cyclopentadienyl fragments together is generation of a cyclopentadienyl radical or radicaloid. In Scheme 3, this is accomplished by oxidation of the cyclopentadienyl anion by

iodine, and in Scheme 4, the coupling is achieved by coordination of Cp^*_2Yb to 4,5-diazafluorene that results in formation of the open-shell singlet ground electronic state of **1**.

The set of elementary reactions outlined in Scheme 4 is consistent with what is currently known about the mechanism. The individual steps are set forth in the sense of a postulate as a guide for further study rather than as an established set of facts. The key postulate, however, is that the electronic structure of **1** stabilizes the biradical enough so that it can be isolated but not so stable that it does not undergo chemistry.

CONCLUSION

Adduct **1** is an example of the growing class of decamethylterytterbocene adducts with 2,2'-bipyridine and its substituted derivatives in which ytterbium has an intermediate valence: that is, its valence is nonintegral and lies between +II and +III. The 4,5-diazafluorene ligand in the adduct is also a radical in which the unpaired spin density is on the π orbitals of the carbon and nitrogen atoms. The electronic structure of the adduct is a multiconfigurational open-shell singlet state that lies 0.55 eV below the triplet state according to CASSCF calculations. In previously reported ytterbocene adducts with open-shell singlet ground states, the biradical adducts are sufficiently stable, relative to the hypothetical triplet biradical, and they do not undergo chemistry. In contrast, the biradical **1** is an example in this class of adducts that is sufficiently stable to be isolated and characterized but is able to undergo chemistry; the heterolytic cleavage of C–H bond generating the Yb(III) amide, **2**, and dihydrogen. Adduct **1** is therefore not just a molecule with unusual magnetic properties; its biradical character also triggers breaking and making chemical bonds.

ASSOCIATED CONTENT

Supporting Information

Figures, text, tables, and CIF files giving information concerning magnetic data, vis–near-IR spectroscopy, kinetics, and X-ray crystallographic data (CCDC 896946 (2) and CCDC 896947 (4)). This material is available free of charge via the Internet at <http://pubs.acs.org>.

AUTHOR INFORMATION

Corresponding Author

*E-mail: raandersen@lbl.gov

Present Address

^{||}Laboratoire Hétéroéléments et Coordination, CNRS, Ecole polytechnique, F-91128 Palaiseau Cedex, France.

Notes

The authors declare no competing financial interest.

ACKNOWLEDGMENTS

This work was supported by the Director, Office of Science, Office of Basic Energy Sciences, and by the Division of Chemical, Geosciences, and Biosciences of the Department of Energy at LBNL under Contract No. DE-AC02-05CH11231. X-ray absorption data were collected at the Stanford Synchrotron Radiation Lightsource, a national user facility operated by Stanford University on behalf of the Department of Energy, Office of Basic Energy Sciences. L.M. is member of the Institut Universitaire de France. Cines and CALMIP are acknowledged for a generous grant of computing time. L.M. would also like to thank the Humboldt Foundation for a fellowship.

REFERENCES

- (1) Booth, C. H.; Kazhdan, D.; Werkema, E. L.; Walter, M. D.; Lukens, W. W.; Bauer, E. D.; Hu, Y.-J.; Maron, L.; Eisenstein, O.; Head-Gordon, M.; Andersen, R. A. *J. Am. Chem. Soc.* **2010**, *132*, 17537.
- (2) Walter, M. D.; Berg, D. J.; Andersen, R. A. *Organometallics* **2006**, *25*, 3228.
- (3) Walter, M. D.; Berg, D. J.; Andersen, R. A. *Organometallics* **2007**, *26*, 2296.
- (4) Walter, M. D.; Schultz, M.; Andersen, R. A. *New J. Chem.* **2006**, *30*, 238.
- (5) Da Re, R. E.; Kuehl, C. J.; Brown, M. G.; Rocha, R. C.; Bauer, E. D.; John, K. D.; Morris, D. E.; Shreve, A. P.; Sarrao, J. L. *Inorg. Chem.* **2003**, *42*, 5551.
- (6) Bordwell, F. G. *Acc. Chem. Res.* **1988**, *21*, 456.
- (7) Booth, C. H.; Walter, M. D.; Kazhdan, D.; Hu, Y.-J.; Lukens, W. W.; Bauer, E. D.; Maron, L.; Eisenstein, O.; Andersen, R. A. *J. Am. Chem. Soc.* **2009**, *131*, 6480.
- (8) Dickeson, J.; Summers, L. *Aust. J. Chem.* **1970**, *23*, 1023.
- (9) Druey, J.; Schmidt, P. *Helv. Chim. Acta* **1950**, *33*, 1080.
- (10) Kloc, K.; Mlochowski, J.; Szulc, Z. *Heterocycles* **1978**, *9*, 849.
- (11) Mlochowski, J.; Szulc, Z. *Pol. J. Chem.* **1983**, *57*, 33.
- (12) Riklin, M.; Von Zelewsky, A.; Bashal, A.; McPartlin, M.; Wallis, J. D. *Helv. Chim. Acta* **1999**, *82*, 1666.
- (13) Allen, F.; Kennard, O.; G., W. D.; L., B.; Orpen, A. G.; Taylor, R. *J. Chem. Soc., Perkin Trans. 2* **1987**, S1.
- (14) Schultz, M.; Boncella, J. M.; Berg, D. J.; Tilley, T. D.; Andersen, R. A. *Organometallics* **2002**, *21*, 460.
- (15) Tilley, T. D.; Andersen, R. A.; Spencer, B.; Zalkin, A. *Inorg. Chem.* **1982**, *21*, 2647.
- (16) Brand, R.; Krimmer, H.-P.; Lindler, H.-J.; Sturm, V.; Hafner, K. *Tetrahedron Lett.* **1982**, *23*, 5131.
- (17) Witte, P. T.; Klein, R.; Kooijman, H.; Spek, A. L.; Polasek, M.; Varga, V.; Mach, K. *J. Organomet. Chem.* **1996**, *519*, 195.
- (18) Stepowska, E.; Huiling, J.; Datong, S. *Chem. Commun.* **2010**, *46*, 556.
- (19) Carlson, C. N.; Kuehl, C. J.; Da Re, R. E.; Veauthier, J. M.; Schelter, E. J.; Milligan, A. E.; Scott, B. L.; Bauer, E. D.; Thompson, J. D.; Morris, D. E.; John, K. D. *J. Am. Chem. Soc.* **2006**, *128*, 7230.
- (20) Boche, G.; Lohrenz, J. C. W. *Chem. Rev.* **2001**, *101*, 697.
- (21) Doering, W. E. *Theoretical Organic Chemistry, the Kekule Symposium*; Butterworths: London, 1959.